Journal of Applied Polymer Science

Dynamic mechanical properties of very thin adhesive joints

Ludovic Krogh,[1] Jürgen E. K. Schawe,[2] Wulff Possart[1]
[1]Saarland University, Chair for Adhesion and Interphases in Polymers, Campus C 6.3-6, PB 151150, D-66123 Saarbrücken, Germany
[2]Mettler-Toledo AG, CH-8603, Schwerzenbach, Switzerland
Correspondence to: W. Possart (E-mail: w.possart@mx.uni-saarland.de)

ABSTRACT: The effective mechanical properties of a polyurethane adhesive (oligoetherdiol, -triol, MDI) in gold joints (bond line thickness, $d_P = 35$–550 μm) are studied in the linear deformation range by dynamic mechanical analysis in shear mode. These properties depend on d_P: thin ones possess a higher dynamic glass transition temperature and show a narrower glass transition than the thick ones. The storage modulus rises with decreasing d_P for the rubbery plateau. The results attest mechanical interphases in the polyurethane with increased crosslink density and reduced cooperative mobility than in bulk. © 2015 Wiley Periodicals, Inc. J. Appl. Polym. Sci. **2015**, *132*, 42058.

KEYWORDS: adhesives; glass transition; mechanical properties; polyurethanes; structure-property relations

Received 22 August 2014; accepted 28 January 2015
DOI: 10.1002/app.42058

INTRODUCTION

It is well known that the viscoelastic mechanical behavior of polymers depends on the rate of deformation and on temperature in a complex way. In polymer-metal joints, an additional complication has to be expected from the adhesion between the polymer and the substrate surface. Generally, any adhesive bonding mechanism immobilizes polymer molecules at the contact to the metal. The adhesive interaction triggers some trend to the demixing of adhesive components and to preferential orientation of adhesive molecules in the region at the contact. Several works have dealt with the formation of resulting interphases in adhesive joints, reporting concentration gradients of the chemical composition in the adhesive at the contact with metal substrate.[1,2]

However, quantitative measurements of such chemical gradients are, in many cases, difficult to perform experimentally and a sufficient local resolution is hard to achieve. Wehlack shows differences in reaction kinetics and chemical conversion of reactive groups between bulk adhesive and adhesive in contact with metal layer on the scale of some hundred nanometers.[3–9] As the result, chemical structure and corresponding network morphology differ in that chemical interphase from the polymer bulk. Consequently, the mechanical properties of that region also differ from the bulk.[10,11]

In addition to the formation of chemical interphases, internal stresses arise in the adhesive as it shrinks during polymerization and vitrification. Krüger *et al.* conclude from Brillouin spectroscopy results on internal stresses in the contact region between the adhesive and the substrate.[12,13] Mechanical modelling reveals the influence of these internal stresses on the formation of mechanical interphases due to polymerization shrinkage.[14–18]

These results lead to the conclusion that the effective mechanical properties of the joint should depend on the adhesive bond line thickness (d_P). For a given combination of adhesive and substrate the thickness rules the volume ratio of interphase and remaining bulk region. Indeed, such thickness dependence was reported for the modulus of selected polymer-metal combinations in the literature.[19–24]

Dynamical mechanical analysis (DMA) would be a promising tool for the analysis of dynamic stiffness and molecular mobility in adhesive joints if accuracy and sensitivity are sufficient. For bonded joints of Al foil with a commercial epoxy network, Caussé *et al.* report a dependence of molecular mobility on d_P within 100 and 600 μm but for only three d_P values.[25] The authors interpret their data as consequence of stiffening that extends from the epoxy-Al contact into the bond line. However, their body of data is limited and the connection between epoxy immobilization at the Al surface and the mechanical behavior remains vague. Moreover, the epoxy composition and the state of curing are not reported in necessary detail. That data encourage extending such measurements. They are needed to model the dynamic mechanical properties of adhesive joints.[26]

In this article, the suitability of DMA is tested further for gold-polyurethane adhesive joints in an extended thickness range. The results give a first characterization of the mechanical

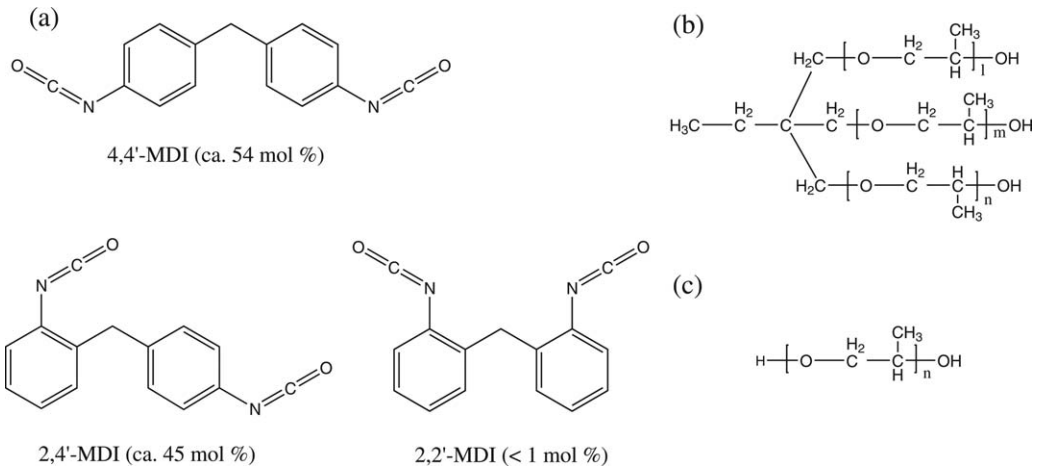

Figure 1. Polyurethane monomers. (a) Methylene diphenyl diisocyanate isomers (MDI), M=250g/mole. (b) Branched polypropylene ether triol, $\overline{l+m+n} \approx 5.3$, $\overline{M} \approx 440$g/mole. (c) Linear polypropylene ether diol, $\overline{n} \approx 34.2$, $\overline{M} \approx 2000$g/mole.

interphases in adhesive joints. They indicate necessary improvements for the experimental technique.

EXPERIMENTAL

To determine the influence of interphases in adhesive joints on their mechanical behavior, gold–polyurethane–gold sandwiches with different adhesive thickness are prepared and mechanically characterized by DMA.

Sample Preparation

Polyurethane Adhesive. The polyurethane adhesive (PU) is made of three monomers (see Figure 1 for chemical structures):

- Methylene diphenyl diisocyanate hardener (a mixture of 54 mole % of 4,4′-MDI, 45 mole % of 2,4′-MDI and <1 mole % of 2,2′-MDI, Bayer MaterialScience AG, Leverkusen, Germany)
- A mixed polyol resin consisting of a linear oligopropylene ether diol ($\overline{M} \approx 2000$g/mole, Bayer MaterialScience AG, Leverkusen, Germany) and a branched oligopropylene ether triol ($\overline{M} \approx 440$g/mole, Bayer MaterialScience AG, Leverkusen, Germany).

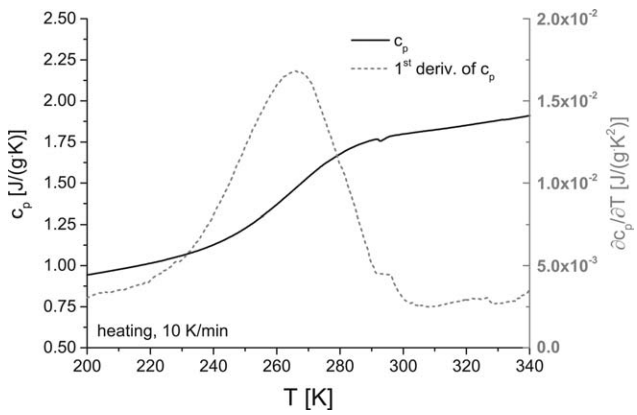

Figure 2. Specific heat capacity $c_p(T)$ measured with DSC during heating with 10 K/min for a cured PU-bulk sample and its first derivative for proper identification of the glass transition range and T_g.

The polyols are mixed at a hydroxyl group ratio of OH_{triol}:OH_{diol} = 80 : 20. The reactive adhesive is prepared as a mixture of the resin and the hardener with a stoichiometric ratio of hydroxyl and isocyanate groups. Full curing to PU is obtained in dried atmosphere by 72 h at room temperature followed by 3 h post-curing at 403 K. The caloric glass transition of the PU ranges from 213 to 303 K (measured by DSC at 10 K/min, Figure 2). The glass transition temperature is $T_g^{DSC,bulk} = 266 \pm 1$ K. Therefore, the PU network is close to the entropy elastic state at room temperature.

Adhesive Joints. The metal substrate is prepared by physical vapor deposition (PVD) of Au (99.99%) on clean glass slides in high vacuum. The compact polycrystalline gold layer has a thickness of about 100 nm. The unreacted adhesive is cast between two substrates. PTFE spacers adjust d_P appropriately between 37 and 550 µm. Due to the poor adhesion between gold and glass, the fully cured adhesive joints are easily separated from the glass slide for DMA measurements (cf. Figure 3 for sample geometry).

Dynamic Mechanical Analysis

Measuring Mode. In material compounds, sample orientation plays an important role for the selection of the optimal measurement mode, for the display of the measured data and hence, for the detection of mechanical effects. This is illustrated in Figure 4 for coatings or laminates where the compound consists of just two components with different mechanical parameters. Obviously, only shear measurements with shear stress along the substrate surface deform the polymer part without significant

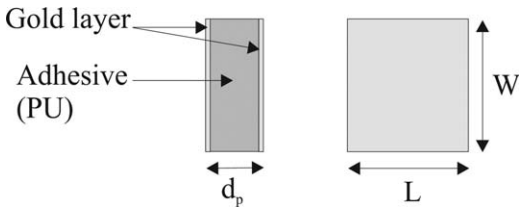

Figure 3. Sample geometry (d_P, sample thickness, including the gold layers; W, width; L, length).

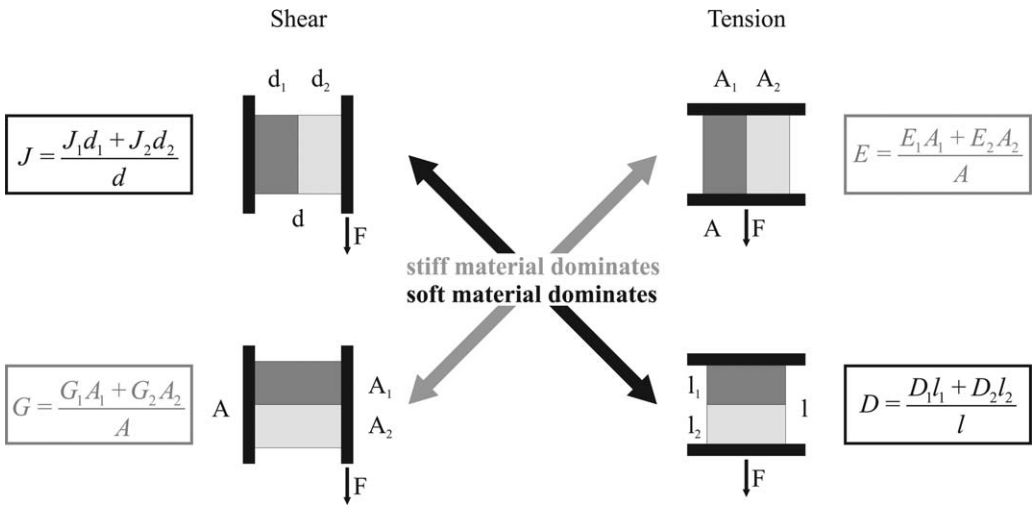

Figure 4. Sketch of the influence of the measuring mode on the measured mechanical properties in the case of bilayered samples. J is the shear compliance, G is the shear modulus, E is the tensile modulus, and D is the tensile compliance.

deformation of the substrates. In the shear mode, the stiffness of thin glassy samples is rather high. Moreover, a high-resolution measurement of small deformation is required to make sure that the material properties are determined in the linear range.

Sample Geometry. DMA is performed with a DMA861^e from Mettler-Toledo AG. This instrument combines a stiffness of about 1.4×10^8 N/m with a displacement resolution of about 0.5 nm. The force generator provides 40 N at maximum. The optimum sample size depends on the material properties of the sample. For definition of the sample geometry, an estimation of the mechanical properties is required. The complex shear modulus, $\hat{G}=G'+iG''$, of a material is proportional to the complex sample shear stiffness, $\hat{S}$

$$\hat{G}=g\times\hat{S} \tag{1}$$

with the geometry factor, g, depending on the thickness, d_P, and the clamped area, A, of the sample:

$$g=\frac{d_P}{2A} \tag{2}$$

Generally, the sample stiffness has to be significantly lower than the stiffness of the instrument, S_i. Otherwise, the measured deformation cannot be attributed to the sample anymore. In the DMA861^e, the maximum sample stiffness should be at least three times lower than S_i. Insertion of eq. (2) in (1) yields an estimate for the maximum sample area, A_{max}:

$$A_{max} \leq \frac{d\times S_i}{6G'_g} \tag{3}$$

with G'_g the storage shear modulus to be measured in the stiffest sample state. Assuming $G'_g \approx 1$ GPa as a typical value of for polymers in the glassy region and $d_P = 40$ µm, we get $A_{max} \approx 1$ mm^2.

Sample Mounting. To double the effective sample thickness, sandwiches of two samples with a plane-parallel steel plate in between (Figure 5) are clamped for those adhesive joints having a thickness below 300 μm. The geometry of the steel plates was A $\approx$ 4 mm^2 and d $\approx$ 350 µm. The sample area was nearly quadratic in the range of 1–3 mm^2. The larger area is used for the thicker samples to get the optimum for the geometry factor for shear samples to avoid sample bending. Furthermore, the clamps have to exert a small but sufficient stress on the sample for shear force transfer.

For such small samples, the external sample preparation, as it is possible with DMA861^e, is necessary.

The shear deformation is given as the deformation amplitude over the effective sample thickness at one side of the shear clamp. Deformation sweep experiments were performed with displacement amplitudes from 1 to 500 nm on samples with 50 to 200 μm PU thickness at room temperature. As the result, a maximum shear deformation of 0.3% was found for linear response. At larger deformations, the samples behave nonlinear, that is, the measured modulus declines with increasing deformation amplitude.

In addition, the shear force amplitude has to be set small enough to limit the shear stress in the case of a stiff glassy sample—the sample would decouple from the shear clamps at too high shear forces. Thus, DMA force amplitude and clap force

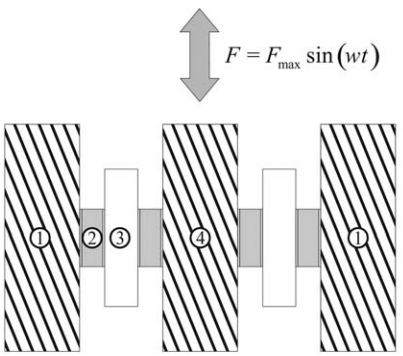

Figure 5. Sample mounting in the shear clamps.

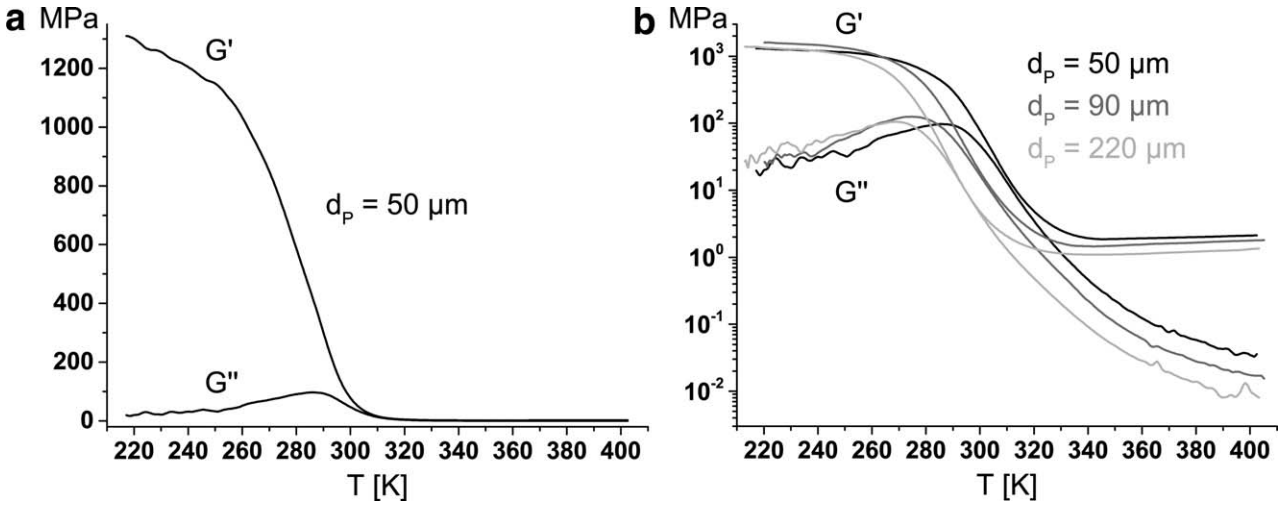

Figure 6. Shear moduli $G'(T)$ and $G''(T)$ at 10 Hz during heating with 4 K/min for gold-PU adhesive joints displayed in the linear (left) and a semi-logarithmic (right) diagram for 50, 90, and 220 μm samples as an example.

have to be chosen carefully. Otherwise for too large shear and compression stresses, the storage modulus grows with decreasing temperature in the glassy region and/or the loss modulus is too high. Appropriate values were determined in screening experiments in the glassy state.

Due to thermal expansion of the samples, the bond line thickness and the sample area vary slightly in the measurement. An estimation of the resulting stress in the sample shows that this effect can be neglected in comparison with the applied small clamping force.

Approach. In the glassy state, the measurement is stress controlled. During heating, the storage modulus decreases and hence, the deformation amplitude grows. To keep the measurement in the linear range the control switches automatically to strain control as the maximum deformation reaches 0.3%.

After mounting shear clamps with the sample, the setup is annealed at 50°C for 15 min in the DMA furnace to eliminate potential internal stresses caused by sample preparation and clamping.

The amplitudes of the sinusoidal deformation and force, as well as the related phase shift are measured for temperature sweeps from 210 to 400 K at a heating rate of 4 K/min. A measuring frequency of 10 Hz was chosen in order to determine a sufficient number of data points under quasi-isothermal conditions at this relatively high heating rate.

RESULTS AND DISCUSSION

The temperature dependent viscoelastic shear modulus $\hat{G} = G' + iG''$ of a 50 µm adhesive joint is shown in Figure 6. The curves represent the dynamic glass transition (α-relaxation) of the amorphous PU-network. The storage modulus decreases by about three orders of magnitude. The G' inflection point at 279 K correlates with the peak maximum of the loss modulus, G''. The rubbery plateau follows above the dynamic glass transition.

According to the interphase and bulk regions in the PU layer, one could expect to see two glass transitions in the modulus curves. This is obviously not the case (Figure 6). Consequently, the measured curves represent the effective mechanical response of the adhesive layer. Therefore, the effective dynamic glass transition has to be analyzed in more detail as a function of PU thickness.

The temperature for the G''-maximum is taken as the dynamic glass transition temperature, $T_g^{\mathrm{dyn},G''}$ for the given frequency of 10 Hz. The thickness dependence is shown in Figure 7.

According to these data, the function:

$$T_g^{\mathrm{dyn},G''}(d_P) = T_1 + \frac{A}{d_P} \tag{4}$$

is chosen for the phenomenological fitting of $T_g^{\mathrm{dyn},G''}(d_P)$. This provides $T_1 = 265$ K and $A = 800$ μm/K. Interestingly, T_1 is equal to the calorimetric glass transition temperature of a bulk sample. Thin adhesive joints tend to a higher value for $T_g^{\mathrm{dyn},G''}$. That dependence indicates an interphase in terms of cooperative mobility in the polyurethane adhesive at the contact with the gold surface. A higher glass transition temperature in thin joints corresponds to a lower mobility of the polymer network chains. As a consequence, one would expect increased mechanical stiffness in a corresponding mechanical interphase.

An equation similar to eq. (4) follows from the assumption of an ideal athermal mixture of bulk and interphase material. This analogy to the well-known DiBenedetto equation[27] is not easy to comprehend for heterogeneous systems as anticipated for the PU adhesive layers. As a first explanation one could assume that the cooperative rearrangement regions average the molecular dynamics.

This view is supported by the thickness dependence of the upper half width of the glass transition, $\left\{T_{\mathrm{end}}^{G''}(d_P) - T_g^{\mathrm{dyn},G''}(d_P)\right\}$, from the peak maximum $T_g^{\mathrm{dyn},G''}(d_P)$ to the upper end of the glass transition $T_{\mathrm{end}}^{G''}(d_P)$ in G'' (Figure 8). The decrease in

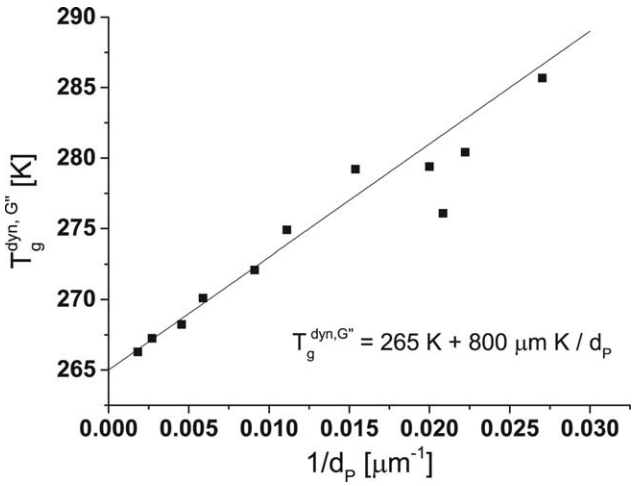

Figure 7. Dynamic glass transition temperature, $T_g^{dyn,G''}$(10Hz) as function of bond line thickness, d_P

$\left\{T_{end}^{G''}(d_P) - T_g^{dyn,G''}(d_P)\right\}$ indicates a reduced variation of segmental mobility inside the mechanical interphase.

The height of the α-relaxation step in log G' from the glassy plateau ($T = 233$ K) to the rubbery state ($T = 353$ K) is presented in Figure 9. The increase of the logarithmic modulus step height with sample thickness is mainly caused by the modulus change in the rubbery plateau.

The height of the G''-peak gives a measure of the mechanical energy dissipated at the glass transition temperature. According to Figure 6, no thickness dependence is obtained within experimental uncertainty.

For an ideal entropic network, that is, $T > T_{end}^{G''}(d_P)$, theory for a Gaussian network with chemical cross-links provides the temperature coefficient for the equilibrium shear modulus G'_{eq} at infinitesimal deformation:[28–31]

$$\frac{\partial G'_{eq}}{\partial T} = \kappa \times R \tag{5}$$

where κ is the molar cross-link density of the polymer and R the universal gas constant.

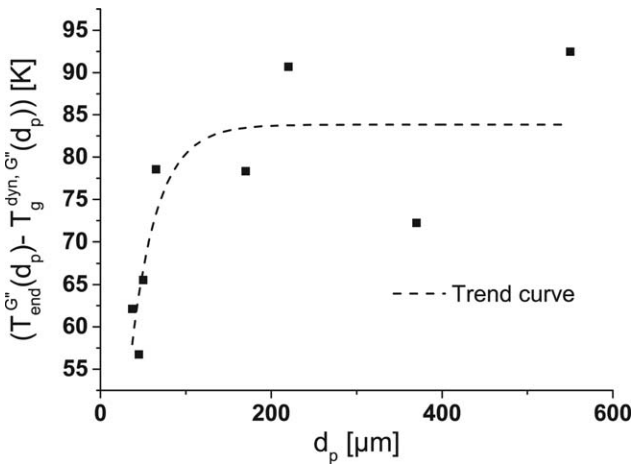

Figure 8. Upper half width of the dynamic glass transition.

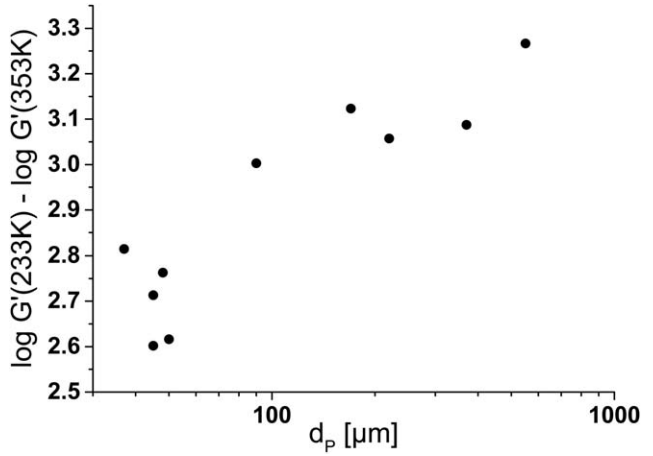

Figure 9. Step height $\Delta \log G' = \log G'(233K) - \log G'(353K)$ as a function of PU thickness, d_P

It is noted in passing that eq. (5) applies to a "perfect" network in that all chains in the network contribute to the elastic stress. In particular, the entropy-elastic network has to be homogeneous in the whole sample and, as a consequence, the κ value obtained from eq. (5) must not depend on the size of the sample. In case of a nonhomogeneous sample, eq. (5) will provide some effective value, κ_{eff}, because the straight line measured for $G'_{eq}(T)$ in fact represents G'_{eq} data averaged over the whole sample volume. Hence, variations of inhomogeneity will result in varying data for κ_{eff}. Actually, the application of eq. (5) to $G'_{eq}(T)$ on the rubbery plateau for the various d_P values of the PU-layer in the Au-joints results in a thickness-dependent effective cross-link density $\kappa_{eff}(d_P)$ (Figure 10). The growth of $\kappa_{eff}(d_P)$ with decreasing film thickness indicates a d_P-dependent inhomogeneity in the PU-layers. In accordance with the picture of a mechanical interphase developed above, we conclude that the deduced κ_{eff} inhomogeneity corresponds to a tighter cross-linking close to the polymer-metal interface. That also explains the higher G' in the rubbery state noted with Figure 6.

With these results, one can check how the cross-link density, κ_{eff} relates to the measured dynamic glass transition temperature, $T_g^{dyn,G''}(d_P)$ (Figure 11).

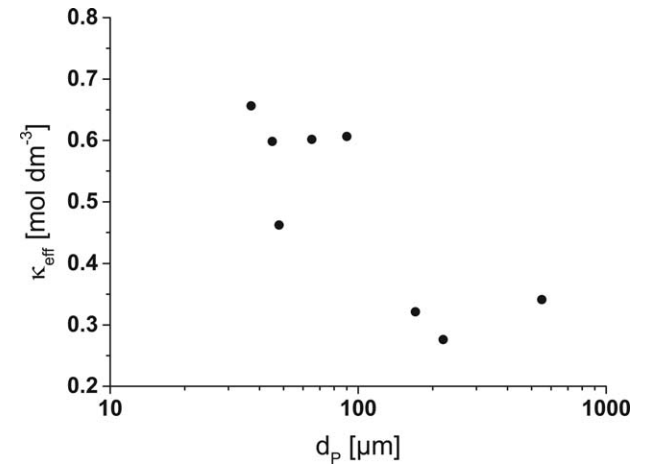

Figure 10. Effective cross-link density, κ_{eff} for Au-PU joints of varying polymer thickness, d_P

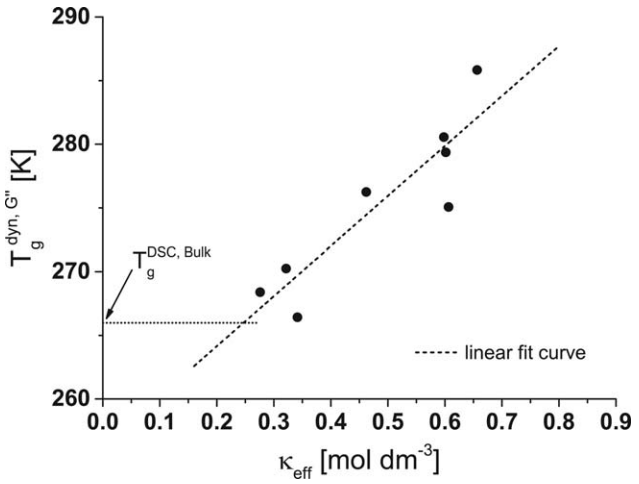

Figure 11. Dynamic glass transition temperature $T_g^{dyn,G''}$ as a function of the estimated effective cross-link density κ_{eff}.

Figure 11 indicates that the glass transition temperature increases approximately linear with the estimated average cross-linking density of the PU film. Hence the bulk glass transition temperature $T_g^{DSC,bulk}$ of 266 K corresponds to an extrapolated $\kappa_{eff} \approx 0.25$ mol dm^{-3}. A crude consideration of the PU network architecture provides an average crosslink density of about 0.4 mol dm^{-3}. Both values are reasonably close to each other with respect to the given level of approximation.

CONCLUSIONS

In the given configuration, DMA is capable to provide good data for metal-polymer-metal sandwich samples down to some 30 µm thickness. For Au-PU-Au samples with a cross-linked PU, the dynamic glass transition parameters as well as the rubber-elastic modulus depend on the sample thickness d_P. These findings are interpreted as the result of a dynamic mechanical interphase of considerable thickness at the polyurethane-gold contacts.

As DMA is averaging over the whole polymer volume, all deduced parameters are mean values that cannot be split easily into contributions from the interphase and bulk regions in the polymer layer of given thickness.

Nevertheless, DMA has the advantage of easy experimental implementation for adhesive joints. In future work, it will be possible to consider the effects of the mechanical interphase as a function of the substrate surface state, of the adhesive composition, of the adhesive joint preparation conditions, etc., provided the sample preparation and thickness are well controlled.

REFERENCES

1. Montois, P.; Nassiet, V.; Petit, J. A.; Baziard, Y. *Int. J. Adhes. Adhes.* **2006**, *26*, 391.
2. Aufray, M.; Roche, A. A. *Int. J. Adhes. Adhes.* **2007**, *27*, 387.
3. Wehlack, C. Chemische Struktur und ihre Entstehung in Dünnen Epoxid- und Polyurethanschichten auf Metallen, Saarbrücker Reihe Materialwissenschaft und Werkstofftechnik; Shaker Verlag: Aachen, Germany, **2009**; Vol. *14*.
4. Wehlack, C.; Possart, W.; Krüger, J. K.; Müller, U. *Soft Mater.* **2007**, *5*, 87.
5. Wehlack, C.; Possart, W. Formation, Structure and Morphology of Polyurethane–Metal Interphases, Proceedings of the 5th International EEIGM/AMASE/FORGEMAT Conference on Advanced Materials Research; IOP Conference Series: Materials Science and Engineering 5, IOP Publishing, **2009**.
6. Wehlack, C.; Possart, W. Interphase Formation, Structure and Properties of Polyurethane Adhesive Networks on Metals, Proceedings of the 4th World Congress on Adhesion and Related Phenomena, Arcachon, France, September 26–30, **2010**.
7. Wehlack, C.; Ehbing, H.; Dijkstra, D. J.; Possart, W. How Do Metal Adherends Influence the Chemical Structure Formation of Thin Polyurethane Films? Proceedings of the 4th World Congress on Adhesion and Related Phenomena, Arcachon, France, September 26–30, **2010**.
8. Wehlack, C.; Mallandain, E.; Ehbing, H.; Dijkstra, D. J.; Possart, W. How Does Air Moisture Affect the Chemical Structure Formation of Thin Polyurethane Films on Metals? Proceedings of the 4th World Congress on Adhesion and Related Phenomena, Arcachon, France, September 26–30, **2010**.
9. Wehlack, C.; Bodin, S.; Ehbing, H.; Dijkstra, D. J.; Possart, W. Properties of Thin Polyurethane Films on Metals at the Glass Transition, Proceedings of the 4th World Congress on Adhesion and Related Phenomena, Arcachon, France, September 26–30, **2010**.
10. Shimizu, K.; Abel, M-L.; Phanopoulos, C.; Holvoet, S.; Watts, J. F. *J. Mater. Sci.* **2012**, *47*, 902.
11. Meiser, A. Vernetzung und Alterung eines Epoxidklebstoffes im Kontakt mit Atmosphären und Metallen, Saarbrücker Reihe Materialwissenschaft und Werkstofftechnik; Shaker Verlag: Aachen, Germany, **2012**; Vol. 31.
12. Krüger, J. K.; Possart, W.; Bactavachalou, R.; Müller, U.; Britz, T.; Sanctuary, R.; Alnot, P. *J. Adhes.* **2004**, *80*, 585.
13. Krüger, J. K.; Müller, U.; Bactavatchalou, R.; Liebschner, D.; Sander, M.; Possart, W.; Wehlack, C.; Baller, J.; Rouxel, D. In Adhesion—Current Research and Applications; Possart, W., Ed.; Wiley-VCH: Weinheim, **2005**, p 125.
14. Hossain, M.; Possart, G.; Steinmann, P. *Comput. Mech.* **2009**, *43*, 769.
15. Hossain, M.; Possart, G.; Steinmann, P. *Comput. Mech.* **2009**, *44*, 621.
16. Hossain, M.; Possart, G.; Steinmann, P. *Comput. Mech.* **2010**, *46*, 363.
17. Mergheim, J.; Possart, G.; Steinmann, P. *Comput. Mech.* **2012**, *53*, 359.
18. Possart, G. Mechanical Interphases in Adhesives-Experiments, Modelling and Simulation, Ph.D. Thesis, Friedrich-Alexander-Universität, Erlangen-Nuremberg, Germany, May **2014**.
19. Schlimmer, M. *Mat.-Wiss. u. Werkstofftech.* **1988**, *19*, 182.
20. Bentadjine, S.; Petiaud, R.; Roche, A. A.; Massardier, V. *Polymer* **2001**, *42*, 6271.

21. Roche, A. A.; Bouchet, J.; Bentadjine, S. *Int. J. Adhes. Adhes.* **2002**, *22*, 431.
22. Possart, W.; Krüger, J. K.; Wehlack, C.; Müller, U.; Petersen, C.; Bactavatchalou, R.; Meiser, A. C. R. *Acad. Sci. Ser. IIc Chim.* **2006**, *9*, 60.
23. Johlitz, M.; Diebels, S.; Batal, J.; Steeb, H.; Possart, W. *J. Mater. Sci.* **2008**, *43*, 4768.
24. Castagnetti, D.; Spaggiari, A.; Dragoni, E. *J. Adhes.* **2011**, *87*, 780.
25. Causse, N.; Quiroga Cortes, L.; Dantras, E.; Tonon, C.; Chevalier, M.; Combes, H.; Guigue, P.; Lacabanne, C. *Int. J. Adhes. Adhes.* **2013**, *46*, 1.
26. Diebels, S.; Geringer, A. *J. Adhes.* **2012**, *88*, 11.
27. DiBenedetto, A. T. *J. Polym. Sci. Part B Polym. Phys.* **1987**, *25*, 1949.
28. Tobolsky, A. V. Mechanische Eigenschaften und Struktur von Polymeren; Berliner Union: Stuttgart, **1967**.
29. Treloar, L. R. G. *Rep. Prog. Phys.* **1973**, *36*, 755.
30. Ferry, J. D. Viscoelastic Properties of Polymers; Wiley: New York, **1980**.
31. Schwarzl, F. R. Polymermechanik-Struktur und mechanisches Verhalten von Polymeren; Springer: Berlin Heidelberg, **1990**.